POLISH MARITIME RESEARCH 2 (122) 2024 Vol. 31; pp. 46-58
10.2478/pomr-2024-0020

Stability Analysis of Dual-Lifting Vessels under Collaborative Lifting Operation

Dejiang Li [1, 2]
ShuMin Li [1, 3]
Qiutong Tan [4 *]
Jiwei Liu [4]
Qiang Fu [5]
Yuhai Sun [1, 5]
Chao Hu [6]
[1] Yantai CIMC Raffles Offshore Ltd., Yantai
[2] CIMC Offshore Co., Ltd (Shenzhen), Shenzhen, China
[3] Faculty of Ocean Engineering Technology, Universiti Malaysia Terengganu, Kuala Nerus, Terengganu, China
[4] School of Ocean Engineering and Technology, Sun Yat-sen University, Guangzhou, China
[5] Shenzhen intelligent Ocean Engineering Innovation Center Co., LTD. Shenzhen, China
[6] College of Shipbuilding Engineering, Harbin Engineering University, Harbin, China

* Corresponding author: *tanqt@mail2.sysu.edu.cn (Qiutong Tan)*

ABSTRACT

The current market for the assembly and disassembly of offshore platforms exceeds $100 billion. However, existing methods face limitations that reduce their efficiency. To address these limitations, we propose a dual-vessel collaborative assembly and disassembly system with multiple motion-compensated lifting arms. The compensation system enables the lifting arms to isolate the topside module from the wave-induced loads, and specifically the torque, transmitted from the lifting vessel. Through theoretical derivations based on hydrostatics principles, a mathematical model of the topside module is established. We consider the effects of lifting load, tidal changes and the ballast water system on stability, and develop a stability analysis model for the dual-vessel system. The intact stability and loss-of-load stability under dual-vessel collaborative lifting conditions are analysed to verify compliance with stability requirements for lifting a 30,000 ton topside module. The results conclusively demonstrate that the proposed system with multiple motion-compensated lifting arms meets the stability performance needs for dual-vessel collaborative offshore assembly and disassembly operations.

Keywords: ship stability; lifting vessel; multi-body system; collaborative lifting operations

INTRODUCTION

The trend towards larger, more integrated marine equipment is driving the offshore construction industry towards collaborative installation practices as the primary operational model [1-4]. Taking platform deployment as an example, we note that the structure is generally divided into two key components: the lower jacket foundation and the topside module. These are typically fabricated separately, and the docking and installation of the topside unit atop the substructure is a crucial but challenging undertaking. The size, weight and functional requirements of offshore platforms lead to varied designs for support structures and modules, each with their own considerations related to installation/removal.

In the early years, the industry's main focus in regard to the installation and dismantling of a platform was to find a lifting ship that could meet the weight and scale requirements of the topside module. The integrated lifting of the upper deck blocks with relatively small scale and weight was completed by lifting equipment positioned on the ship. The capabilities of vessels have been continually increased to accommodate the growing infrastructure. Shanghai Zhenhua's 240 m *Blue Whale* [5,6] (Fig. 1(a)) entered service in 2008, offering 7,500-ton lifting, whereas their 2016-delivered *Zhenhua 30* [7] (Fig. 1(b)) lifted 12,000 tons, with a length of 320 m. Heerema and Sembcorp launched the semi-submersible crane vessel *Sleipnir* [8] (Fig. 1(c)) in 2019, which was equipped with dual revolving cranes providing 20,000-ton lifting via a dual-lift configuration.

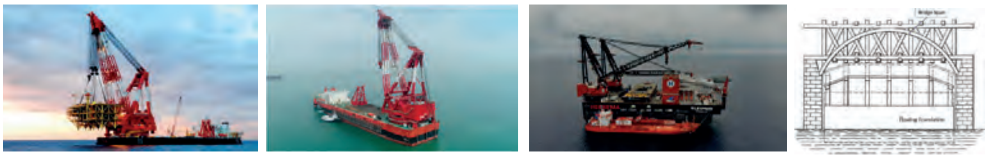

(a) (b) (c) (d)

Fig 1. (a) Blue Whale (COOEC) [7,8]; (b)Zhenhua 30 (ZPMC) [7]; (c) semisubmersible Sleipnir(HMC) [8]; (d) bridge installation method of John Du Bois (US Patent 36606) [9]

As demand for deep-water oil and gas development has increased, the scale and dimensions of offshore platform topside modules have likewise expanded significantly. In parallel with further developments in the specifications of heavy lift vessels, alternative integrated installation methods that are not wholly reliant on a single vessel's maximum lifting capacity have also drawn attention. One early inspiration was an 1862 patent for a process of installing bridge structures, which foreshadowed later developments in the float-over technique that is now common in marine engineering projects [9]. As depicted conceptually in Fig. 1(d), this approach involved floating key structural elements into position rather than hoisting them via crane. This pioneering work highlighted the potential for collaborative, multi-unit solutions to tackle the challenges of infrastructure installation posed by the ever-growing specifications for topside modules.

Aker, a US firm, developed a movable rod lifting system known as the VERSATRUSS technique. Using tension rods, hoists and support rods positioned across two construction barges, this system enables the lifting of modules of up to 10,000 tons in shallow waters with small air gaps between the surface and load [10,11]. However, this method is subject to environmental and dimensional constraints. Another solution, the VB10000 Versabar lifting crane, consists of a heavy-duty double gantry catamaran design with two 91 m truss frame barges, each capable of 7,500-ton lifting [12]. Dynamic positioning systems maintain the positioning of the barges during operations. Although this offers expanded capabilities compared to single-vessel options, limitations remain in terms of block dimensions and weight, due to the intrinsic configuration of these multi-barge collaborative systems. Both of these innovative approaches rely on the concept of distributed lifting forces across two or more purpose-built units.

A mainstream solution based on a 10,000-ton floating installation emerged in the late 1970s. In 1979, its first offshore application involved installing the 6,500-ton topside module onto the Zakum jacket platform in Abu Dhabi [13]. Then, in 1980, Abbot developed the HIDECK float-over methodology [14], as illustrated in Figs. 2(c) and (d) [15]. Although first applied to Maureen's gravity platform, its principles apply similarly to fixed jacket structures. Related patents proliferated between 1980 and 1981 [16,17]. Subsequently, Technip developed the UNIDECK float-over technique, in which hydraulic lifting was used to rapidly transfer the module mass to the foundations between wave periods, thereby avoiding collisions from excessive heave [18-20]. A detailed comparison of UNIDECK and HIDECK was conducted by Liu and Li [21]. Today, the world's most advanced installation/removal vessel, *Pioneering Spirit*, uses a double-sided bow lifting arm configuration based on UNIDECK principles [22,23], as depicted in Fig. 2(f). The docking time has been reduced from hours with HIDECK/UNIDECK to just seconds through the use of collaborative dual-arm operations.

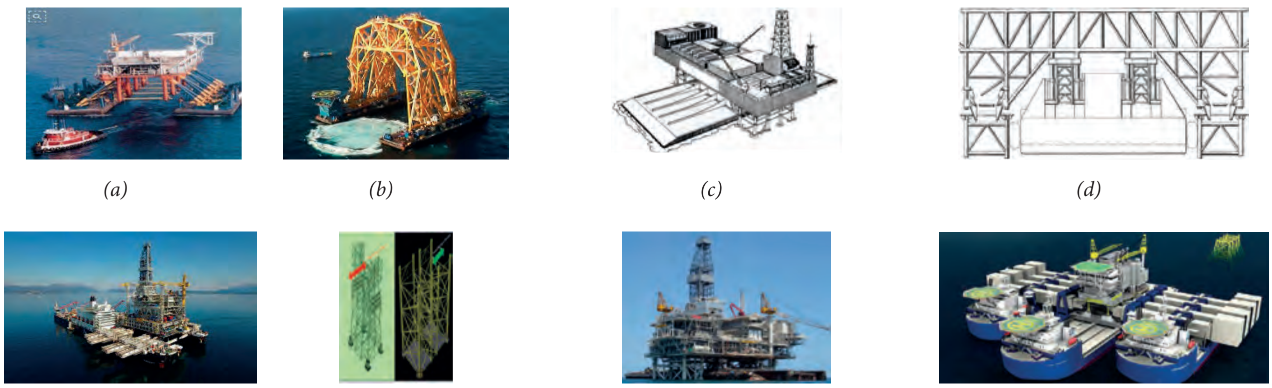

(a) (b) (c) (d)

(e) (f) (g)

Fig. 2. (a) VERSATRUSS hoist system[10, 11]; (b) VB10000 hoist system [12]; (c) HIDECK floating installation concept (OTC3978) [15]; (d) HIDECK floating installation concept [15];(e) Pioneering Spirit (Allseas) [23]; (f) ACG Caspian floating installation of a topside module jacket platform in a sea area [24]; (g)Catamaran collaborative operation [25]

Although extremely heavy lifting vessels can conduct float-over installations independently, multi-vessel cooperative operations have emerged as a novel methodology. These typically involve three barges, with one acting as a transport unit and two collaborating in float-over activities. As distinguished from fixed-jacket foundations, where docking is carried out solely by ballast manoeuvres of the support unit/structure, multi-vessel cooperation involves synchronised control challenges during offshore execution. If the topside module is transferred from the transport to two float-over installation barges in a rigidly connected configuration, the entire structural system resembles the bow U-notch configuration of *Pioneering Spirit*, and is known as a catamaran due to its two-hull form, as illustrated in Fig. 2(g) [25]. The catamaran mode allows for active distance adjustments between vessels to accommodate modules of varying dimensions. However, rigidly connecting these modules introduces structural loading complexities, as loads are directly transmitted to potentially fragile, aging modules that are not designed to withstand such dynamic offshore stresses, and this is a significant design consideration.

There are several limitations on current offshore installation and disassembly equipment, for example: (i) existing lifting ships have low lifting capacity, and large modules need to be divided into many segments for disassembly operations, resulting in long operation times and high risk; (ii) when the barge floating mode is used, operation is greatly affected by the tide; (iii) topside modules with large air gap heights impose requirements for the selection of barge dimensions; (iv) the U-groove mode of operation is limited by the size of the block, the equipment cost is very high, and the operational flexibility is insufficient; and (v) the use of the catamaran mode of operation presents a huge challenge in terms of the strengthening of old oilfield facilities.

To address these existing challenges, this study proposes a novel dual-vessel cooperative assembly/disassembly system that involves multiple motion-compensated lifting arms. Through theoretical modelling based on static principles, a mathematical representation is derived to characterise the model of the lifted topside module. A distinguishing feature is the implementation of a compensation mechanism that isolates the bending moments at the module-lifting interface. This mitigates the transmission of wave loads, and particularly wave-induced torques, from the lifting vessel to the lifting arms and topside module. Variations in lifting load, tidal fluctuations, and ballast conditions are considered, and rigorous stability analyses are conducted to assess the intact and loss-of-load stability under collaborative heavy lifting operations. The compliance of our system with the relevant standards is numerically validated.

TYPES OF CONNECTION AND SIMULATION OF A MULTI-FLOATING BODY OPERATION SYSTEM

The operation of the dual-vessel lifting arm process is as follows. Multiple sets of lifting arm systems are installed on each of the two lifting vessels, positioned on opposing sides of the target object. Hydraulically actuated bearing components are located at the distal ends of the arms to enable lifting and lowering of the target through precise adjustments that are coordinated with ballast water trim. Long-distance transport is facilitated via a dedicated third barge. In addition to dismantling aging platforms, the system is equally capable of installing new modules by directing lifting/offloading to alternate docking positions as required. Fig. 3 provides an analytical schematic depicting sample configurations during dismantling operations, and illustrates the spatial layout of the HLV1 (Heavy Lifting Vessel 1), the HLV2, the target object (e.g. topside, jacket), and the CV3 (Carrier Vessel 3).

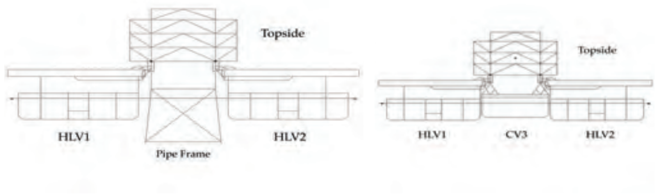

(a) *(b)*

Fig. 3. (a) Lifting conditions, showing the layout of HLV1 + target (topside module and jacket) + HLV2; (b) unloading condition, the layout of HLV1 + CV3 + HLV2

Dual-vessel cooperative lifting operations differ in a fundamental way from single-ship heavy lifting by virtue of their increased complexity. For single-vessel lifts, we only consider the stability of the vessel and crane load capacity, whereas collaborative lifts necessitate an analysis of the loads on the lifted topside module along with the intact stability of both the lifting vessels and the integrated system as a whole.

In general, there are two types of connection between the topside module and lifting vessels. One is a rigid connection, in which all components are structurally welded to form a unified whole, while the other relies on a motion compensation system that provides a degree of freedom, approximating a hinge-like connection.

Table 1 compares the hydrostatic parameters of the stability models for the two connection modes. It can be seen that the stability parameters differ noticeably between the rigid and hinged configurations.

Fig. 4 shows the hydrostatic table corresponding to the rigid connection model, and Fig. 5 presents the coordinate system for the hydrostatic models. Fig. 6 illustrates the hydrostatic models for a 16 m draft.

Tab. 1. Comparison of hydrostatic parameters of stability model for two connection modes

Connection type	Draft (m)	Total drainage volume (m3)	Total displacement (ton)	LCF (m)	LCB (m)	GMT (m)	GML (m)
Rigid	16	399,496	409,483	109	111	227	292
Hinge form	16	199,667	204,658	109	111	32	292

T m	VOLM m3	VOLT m3	DISP t	LCA m	LCB m	VCB m	KMT m	KML m	TPC t/cm
15.2	376341	376993	386417	108	111	8.12	238	304	287.5
15.3	379145	379799	389294	108	111	8.17	236	302	287.7
15.4	381952	382607	392172	108	111	8.22	235	300	287.9
15.5	384760	385417	395052	109	111	8.28	234	299	288.2
15.6	387570	388229	397934	109	111	8.33	232	297	288.4
15.7	390382	391042	400818	109	111	8.38	231	296	288.6
15.8	393197	393858	403705	109	111	8.43	229	295	288.8
15.9	396013	396676	406593	109	111	8.49	228	293	289.0
16.0	398831	399496	409483	109	111	8.54	227	292	289.2
16.1	401651	402318	412376	109	111	8.59	225	290	289.4
16.2	404473	405141	415270	109	111	8.64	224	289	289.6
16.3	407297	407967	418166	109	111	8.70	223	288	289.8
16.4	410123	410795	421064	109	111	8.75	222	286	290.0
16.5	412951	413624	423965	109	111	8.80	220	285	290.2
16.6	415781	416456	426867	109	111	8.86	219	284	290.4

Fig. 4. Hydrostatic table for the rigid connection modelFig. 5. Coordinate s

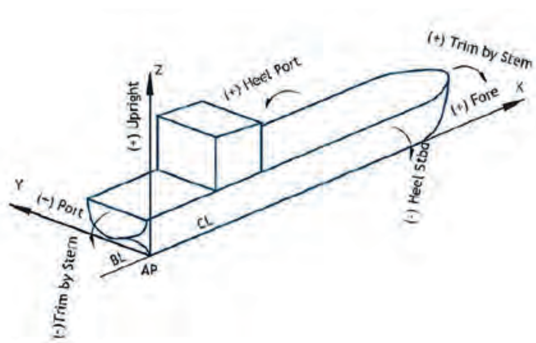

Fig. 5. Coordinate system for hydrostatic models

As illustrated in Fig. 6(a), with a rigid connection, the lifting arm binds the topside module to both lifting vessels, forming a unified whole where the parts are incapable of independent motion. This integrated system resembles a semi-submersible platform with a double-hull form, and in a stability modelling analysis, it can be treated as a catamaran and assessed in the same manner. Table 1 provides the key hydrostatic parameters for evaluation, of which the transverse and longitudinal stability centre heights are particularly important metrics. With a rigid arm connection, the longitudinal stability centre height is 292 m as compared to a transverse height of 227 m, with both being on the same order of magnitude. This connection approach thus confers strong longitudinal and transverse stability for heights that are well above the waterline.

With the rigid connection method, the wave load acting on the two lifting ships is completely transferred to the lifting system and the topside module via the rigid connection between the lifting system and the topside module, which imposes high requirements for the structural strength of the topside module. In practice, the initial design of the topside module does not consider the need to bear the part of the load generated by the movement of the lower floating body.

In contrast, a hinged connection allows the lifting arm, topside module and vessels to behave as three independent bodies with relative movement, although this is somewhat constrained. Consequently, the bending moments induced by ship motions are released at hinge points. For stability analysis, the system can thus be decomposed into the individual floating bodies (the two vessels and the lifted module) for evaluation of the intact stability. As shown in Fig. 6(b) and Table 1, when modelling a single vessel, the height of the lateral system stability centre is a mere 32 m when hinged, much lower than the longitudinal height of 292 m, meaning that lateral stability across the entire cooperative system is relatively weak.

Hence, after comparing and analysing the characteristics of the two connection forms, it is found that although a rigid connection has very high stability and safety, it is very difficult to realise in actual marine engineering, especially for the dismantling of old platforms, due to stiffness and strength problems. An approach based on a lifting arm motion

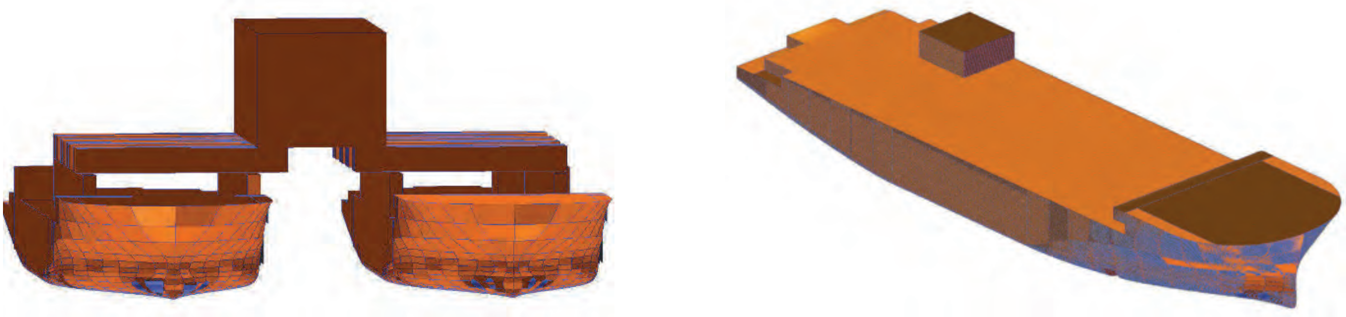

(a) (b)

Fig. 6. Stability models for rigid and hinged connections: (a) hydrostatic model for a rigid connection; (b) hydrostatic model for a hinged connection

compensation system is therefore proposed. Through the action of the compensation system, the bending moment at the connection between the lifting system and the topside module is released, and load from waves acting on the lifting ship (and especially the torque) is avoided, as it is transmitted to the lifting arm and the topside module, thus ensuring the structural integrity of the topside module. However, the way in which the resulting multi-body system provides sufficient stability and safety, its evaluation and the method used for analysis need further study.

PRINCIPLE OF ANALYSIS OF COLLABORATIVE LIFTING OPERATION

For the hinged configuration shown in Fig. 7, preliminary evaluations suggest that without corrective measures, the lifting of a topside module would induce an overturning moment in a single lift vessel, causing a static heel angle exceeding 15°. This inclination would prevent the targeted lift height from being achieved, while also potentially damaging the lifting equipment. To balance this substantial rolling moment produced by the weight-arm lifting, precise ballast transfers are required within the lift vessel during its operation. The internal repositioning of ballast is done with the aim of maintaining safe intact stability in the vessel, as it interacts dynamically with the lifted module as an integrated multi-body system. Without real-time compensation of the heeling forces via the ballast system, safe collaborative offshore lifts would not be feasible, given the excessive motions and stresses on equipment and infrastructure that would otherwise result. Hence, in order to provide sufficient lifting capacity, there is a need for real-time monitoring and adjustments to the internal ballast distribution network as a critical active control method for counteracting rolling incidents induced at the unique motion-constrained connection points between the floating bodies under the hinged configuration.

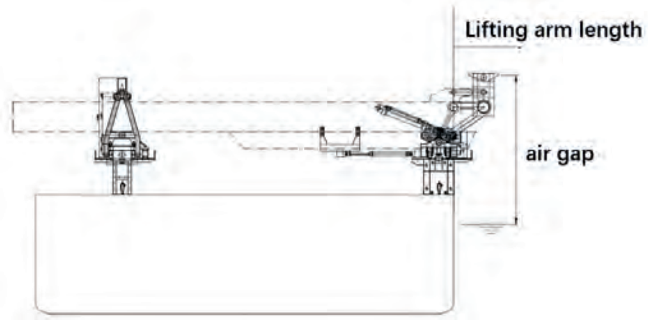

Fig. 7. Diagram of the lifting arm overhang

Reliable and efficient ballast management is paramount to achieving both the lifting function and overall system stability under dynamic offshore conditions. In the following section, we use static equilibrium principles to analyse the moment variations that occur throughout the lifting process.

LIFTING LOAD STOWAGE

Prior to initiating the lift, it is imperative to maintain positive stability. At this pre-engagement stage, minor ballast water adjustments suffice to counteract any deviations in the lifting arm's centre of gravity from its ideal aligned position, thereby minimising incipient rolling moments. However, as the arm extends outward, its centre of gravity shifts correspondingly, inducing an increasing heeling torque upon the vessel. Precise ballast redistribution is thus necessitated to prevent undesirable heel and retain upright equilibrium. Through analytical modelling of the load balance preservation process arising from ballast regulation at each phase of the arm's movement, from retraction to full extension, the overturning moment directly correlating with arm lengthening can be derived.

It is assumed that the centre of gravity of the lifting arm is in position y_1 before it is extended. When the lifting arm extends outboard, it reaches a position y_2. This process of overhanging will cause the ship to heel.

The overhang of the lifting arm on the ship is equivalent to the movement of a heavy object on the ship. From statics, we know that the moment causing the ship to tilt is:

$$M_h = \Delta\overline{GM}\phi \tag{1}$$

where Δ is the displacement of the ship and can be obtained from the weight of the ship and the hydrostatic curve; and ϕ is the heeling angle of the ship caused by the load, which is the high initial stability of the ship, and is obtained by the following formula

$$\overline{GM} = \overline{KB} + \overline{BM} - \overline{KG} \tag{2}$$

$$\overline{BM} = \frac{I_T}{\nabla} \tag{3}$$

$$p_0(y_2 - y_1) = \Delta\overline{GM}\tan\phi \tag{4}$$

$$\Delta\overline{GM}\tan\phi = M_{ballast\ water\ for\ lifting\ arm} \tag{5}$$

where $(y_2 - y_1)$ is the vertical distance moved by the centre of gravity of the lifting arm along the ship's width, and p_0 is the weight of the lifting arm. Using the formula above, the overturning moment generated when the lifting arm of the ship is extended can be calculated. Since $\overline{GZ} = \overline{GM}\tan\phi$ at small angles, GZ does not appear in the equations presented here. The overturning moment generated by the lifting arm will be balanced by the transfer of ballast water.

By redistributing ballast water, the overturning moment induced by extension of the lifting arm is counteracted, establishing a new positive metacentric height for the crane vessel that is sufficient for the subsequent lift stages. An evaluation of the minimum duration of ballast shifting must account for the individual tank volumes, centroid locations, and positions of the centre of gravity of loads, in conjunction with each tank's hold capacity. The overall system capabilities, including the maximum shifting rate and total shift volume, must also be characterised. Through analytical modelling incorporating these constraints and considerations, an optimised ballasting approach can be developed to precisely manage the stability challenges within the timescales demanded by heavy lifting operations.

Maintaining a state of positive equilibrium for the crane vessel throughout the load transfer process is imperative to ensure the safety of operations. As expressed in the theoretical equation provided above, the change in rolling moment caused by incremental load additions must necessarily equal the rolling moment generated by the regulation of ballast water, as follows:

$$M_{Cargo} = M_{ballast\ water\ for\ cargo} \tag{6}$$

It is assumed that the position of the lifting head during the lifting process is y m from the mid of the ship, and that the overturning moment increases with the lifting load w. The torque M_y generated by the lifting load can be expressed as:

$$M_Y = wy \tag{7}$$

The torque generated by an increase in the lifting load will be balanced by the ballast water allocation of the ballast water system. The transverse distance between the port and starboard heeling tanks participating in the load adjustment is L_y, and the transverse ballast water allocation Q_y can be obtained by the following formula:

$$Q_Y = \frac{M_Y}{L_Y} \tag{8}$$

Assuming that the flow rate of the ballast pump is q and the amount of water to be adjusted is Q , the load adjustment time t of the ballast water is shown in Eq. (9):

$$t = \frac{Q}{q} \tag{9}$$

The maximum ballast water transfer volume Q (transferred from the port ballast tanks to the starboard ballast tanks) is approximately 10,900 m^3. A single vessel is equipped with seven groups of anti-heeling tanks and a total of 14 anti-heeling pumps. The flow rate of each pump q is 1,500 m^3/ h.

INFLUENCE OF THE TIDE ON HULL BALLAST WATER ADJUSTMENT

When modelling the lifting process, tidal influences on hull loads must be considered in addition to the module weight. For dismantled topside assemblies that are initially fixed to jackets, the seabed interface height remains fixed, while the sea level fluctuates with the tide. We adopt conservative assumptions, and hypothesise that load transfers during lifts require maintenance of elevation relative to the seabed rather than the sea surface, absent tidal assistance. Thus, the ballast water system capacity must accommodate tidal variances. Precise adjustments to ballast volumes can mitigate tidal impacts, whereby ballast is increased during flood tides and decreased during ebb tides. This stabilises the unchanging differential in elevation between the vessel and seabed throughout lifts. Ensuring this constant relative positioning facilitates a smooth load transfer sequence between the lifting arms and payloads.

The regulation of ballast water can be determined according to the tidal information of the sea area of operation and the variation of the unit cm drainage tonnage of the lifting vessel. It is assumed that the tidal change is h m, and for variation TPC of the drainage tonnage per cm of a single ship, the ballast water required to be discharged or loaded during the adjustment process is:

$$Q_w = 100 \cdot TPC \cdot h \tag{10}$$

BALLAST WATER SYSTEM MATCHING

Based on prior research into load stowage optimisation and the assessment of tidal influence, dual-vessel cooperative heavy lifts require consideration of both the load transfer sequencing and tidal impacts to adequately prepare for variance between sea areas. When we factor in the moment induced by increasing payloads, we see that vessel heeling tends to develop. To control this inclination, a transverse load equalisation system is installed to enable coordinated ballast water reallocation in reverse, thereby achieving the object of load transfer while preserving a positive equilibrium. Lifting vessels are thus outfitted with ballast plants capable of both assembly and disassembly operations. Through precise control, the ballast system ensures that the relative elevation between the lifting vessel and topside module remains essentially unchanged throughout the entire load transfer process.

In order to achieve the above functions, we set up seven pairs of side cabins on the lifting vessel, as shown in the ballast tank layout diagram in Fig. 8: the heeling cabin, the port layout heeling cabin (represented as 2P), and the starboard heeling cabin (represented as 2S), which is used for the ballast transfer of load transfer during lifting. These heeling tanks are distributed on both sides of the hull. The regulating water can be transferred from the heeling tank on one side to the tank on the other through the heeling pump, to realise the internal transfer of the regulating water, thus increasing the regulating force arm and the restoring moment to the greatest extent in the limited space on board the ship. The transverse tilting tanks are deep tanks extending from the bottom of the ship to the top of the main deck, to increase the amount of water and the moment of reloading. The lifting ship is equipped with ballast tanks, which are represented as 1P, 1S and C (indicating the port, starboard and intermediate ballast tanks, respectively). During the lifting load transfer process, these ballast tanks are loaded and discharged with external seawater through the ballast system in order to adapt to tidal changes.

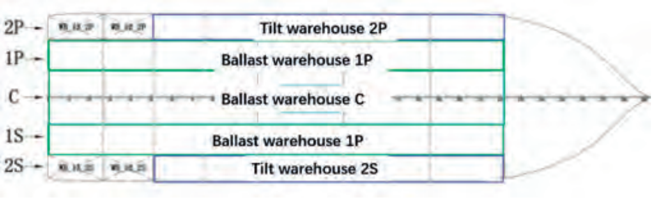

Fig. 8. Layout of the ballast tanks of the lifting ship

Fig. 9 shows a schematic diagram of the lateral section of the ballast tank. The initial ballast water condition, the ballast water adjustment between the 2S and 2P heeling tanks, the tidal adjustment of the ballast water condition of the ballast tank, and the real-time changes are used to reflect the changes in the ballast water volume of each cabin during the operation.

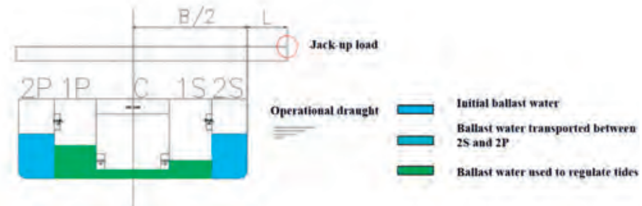

Fig. 9. Horizontal section diagram of the ballast tank

In order to more clearly describe the relationship between the load transfer and the change in the ballast water during the lifting operation, Fig. 10 shows the ballast water changes of 5%, 95%, 100% of in the transverse ballest warehouse during the lifting and lowering processes. The process of ballast water in the left and right two transverse ballest warehouse to achieve load transfer, and the operational draught remains unchanged.

Fig. 11 provides schematic representations of the variations in ballast tank volumes over the high and low tidal stages. Calculations are conducted based on the tidal datum specific to the project area to quantify the ballast demand for an entire tidal cycle. This ensures sufficient ballast reserves and tankage when establishing the starting load conditions. At high tide, pumps convey seawater into tanks, causing a concurrent rise in draught. Conversely, low tides necessitate tank deballasting to lower the draught via controlled discharge overboard.

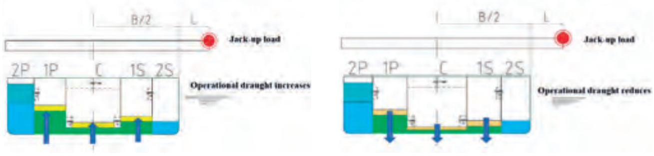

(a) *(b)*

Fig. 11. Schematic diagrams showing the change in ballast tank water volume at: (a) high tide; (b) ebb tide

Through analytical modelling of the overturning moment induced by the lifting arm and lifted payload, and accounting for the tidal influences integral to the disassembly activities, an optimised design solution was obtained. The ballast compartment layout and system capacity were matched to stabilise the lifting vessel configuration for varying operational load cases.

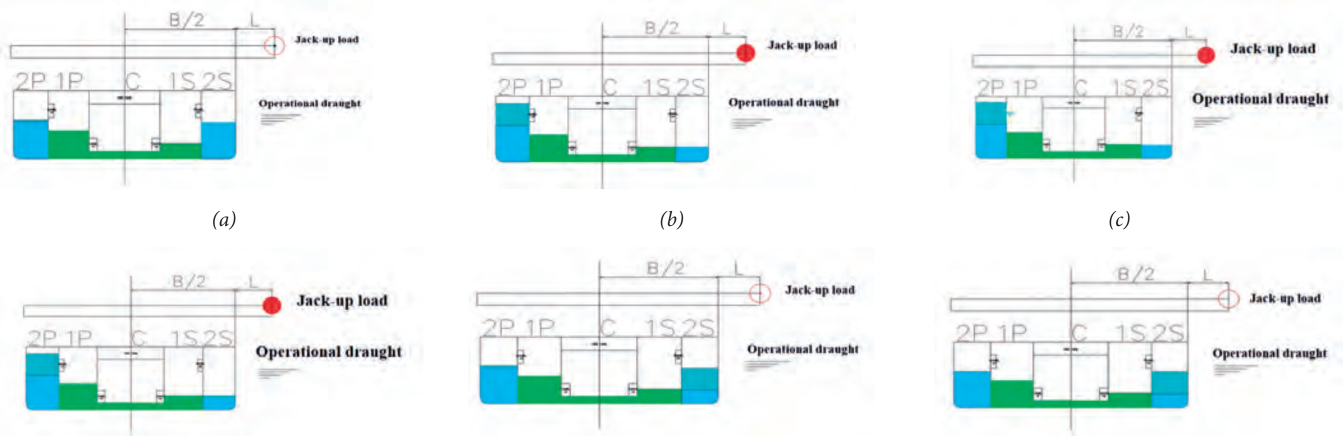

(a) *(b)* *(c)*

(d) *(e)* *(f)*

Fig. 10. Schematic diagrams of the ballast water changes in the transverse ballest warehouse during the lifting and lowering processes: (a) loading 5%; (b) loading 95%; (c) loading 100%; (d) unloading 5%; (e) unloading 95%; (f) unloading 100%

STABILITY ANALYSIS OF THE TOPSIDE MODULE

Through a comparative assessment of the rigid and hinged interfacing between the topside module and dual lifting vessels, a motion-compensated lifting arm configuration mimicking a hinged connection was selected for the integrated operational system. The overall stability of the multi-body collaborative approach is markedly influenced by the intactness or loss-of-load stability states of the lifted module. Further analytical investigation is therefore required to resolve how the motion of the module affects the equilibrium of the lifting vessel for all potential load cases.

The stability state diagram in Fig. 12 shows the ultimate tilt state of the topside module. At this time, the two lifting vessels are in a synchronous right roll tilt state. The lifting head of the left lifting vessel is downward, and that of the right lifting vessel is upward, so that the topside module produces the maximum left roll tilt state. Conversely, when the two lifting vessels are in reverse roll tilt, the lateral tilt state of the block is relatively small. The limiting tilt state is therefore selected as an example to study the stability analysis method of the topside module.

For the topside module, the two lifting vessels are equivalent to two springs that provide stiffness support, and this system can be simplified as shown in Fig. 13.

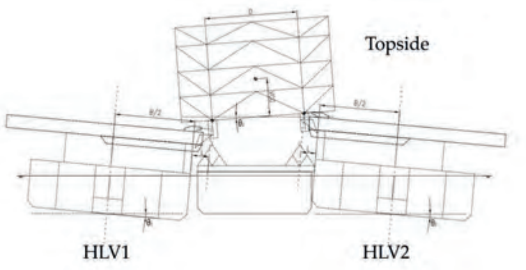

Fig. 12. Stability state diagram for the multi-body system

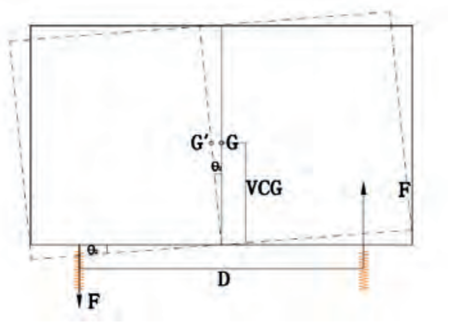

Fig. 13. Force diagram of the topside module

In the multi-body system, the topside module, as an independent entity, has its own instability. Even in still water, the topside module will have a tendency to tilt, and a small disturbance from the outside will cause it to tilt. When this inclination occurs, the centre of gravity G of the topside module is shifted from its original position to G', producing an inclination angle θ_2. In order to maintain balance, the two spring support points will produce a pair of couples $M(F, F')$. The force F reversely acts on the HLV_1 and increases the lateral overturning moment. For the HLV_2, this is equivalent to reducing the lateral overturning moment. If the stiffness provided by the lifting vessel to the topside module is insufficient, the topside module will become unstable; in order to ensure the stability of the topside module, the crane must provide sufficient stiffness, as determined by the GM value for the ship that determines the draught. Hence, the stability of the topside module can be quantified by the GM value of the lifting vessel

The increased force F of the topside module tilted to the lifting vessel

$$F = \frac{W \cdot sin\,\theta_2 \cdot VCG}{D} \tag{11}$$

The overturning moment from the topside module on the lifting vessel is

$$M_H = F \cdot \left(L + \frac{B}{2}\right) \tag{12}$$

The relationship between the ship inclination θ_1 and block inclination θ_2 is

$$sin\,\theta_2 = 2(\frac{B}{2} + L) \cdot \frac{sin\,\theta_1}{D} \tag{13}$$

Hence, the overturning moment generated by the block is

$$M_H = VCG \cdot W \cdot \frac{sin\,\theta_2}{D} \cdot (\frac{B}{2} + L) \tag{14}$$

or

$$M_H = VCG \cdot W \cdot \frac{sin\,\theta_1}{D^2} \cdot (\frac{B}{2} + L)^2 \tag{15}$$

The restoring force moment can then be expressed as:

$$\begin{aligned} M_R &= \Delta \cdot GM \cdot sin\,\theta_1 - VCG \cdot W \cdot \frac{sin\,\theta_1}{D^2} \cdot 2(\frac{B}{2} + L)^2 \\ &= \Delta \cdot sin\,\theta_1 \cdot (GM - VCG \cdot W \cdot \frac{1}{\Delta g D^2} \cdot 2(\frac{B}{2} + L)^2) \end{aligned} \tag{16}$$

In the formulae above, M_H is the overturning moment, M_R is the restoring force moment, θ_1 is the ship tilt angle, θ_2 is the inclination angle of the topside module, W is the total weight of the topside module, VCG is the vertical center of gravity of the topside module, D is the lifting point spacing, B is the breadth of the ship, L is the overhanging outboard distance of the lifting arm, Δ is the displacement, and GM is the initial stability is high.

The term $VCG \cdot W \cdot \frac{1}{\Delta \cdot D^2} \cdot 2(\frac{B}{2} + L)^2$ in Eq. (16) is an important parameter that affects the restoring moment of the system. It can be regarded as the minimum requirement for the topside module for the lifting vessel, and is called the stability of the topside module. This minimum *GM* requirement can also be understood as the correction of the stability of the lifting vessel by the topside module in the stability analysis of the multi-body system, that is, the stability correction term for the lifting vessel δGM.

$$\delta GM = VCG \cdot W \cdot \frac{1}{\Delta \cdot D^2} \cdot 2(\frac{B}{2} + L)^2 \tag{17}$$

From the above derivation, the influence of the topside module on the stability performance of the whole lifting operation in the multi-body system can be decomposed into two parts: the static load of the topside module borne by the lifting vessel, and the overturning moment caused by the dynamic inclination of the topside module. The static load of the topside module borne by the lifting vessel is balanced by the transfer of ballast water from the left and right side heeling tanks, while the overturning moment caused by the dynamic inclination of the topside module requires the displacement of the lifting vessel and high initial stability to provide the restoring moment to reach a balance.

STABILITY ANALYSIS OF THE MULTI-BODY COLLABORATIVE OPERATION SYSTEM

When conducting a stability analysis of the multi-body floating system, the load from the topside module acting on the lifting system, the self-weight of the lifting system, and the load distribution of the lifting system are considered and transformed into a point load on the hull, and calibration is carried out by establishing a stability model of the hull and analysing the relevant stability indexes for the hull.

The overturning moment generated by the inclination of the topside module is reflected in the stability analysis. There are two possible approaches: one is to convert the overturning moment to the VCG of the topside module, which is reflected by increasing the VCG of the topside module; the other is that overturning moment be added to the loading calculation in the form of a free surface inertia moment.In this study, a stability analysis of the multi-body system is carried out based on the free surface inertia moment. The free surface inertia moment can be expressed as:

$$FSRM = \delta GM \cdot \Delta \tag{18}$$

By modelling the lifting vessel, the contours of the wind area and the design water inlet point are established, and the stability performance of the multi-body system is analysed based on the applicable stability evaluation criteria. Table 2 shows the main dimensions of the lifting vessel used in the multi-body collaborative operation system.

Tab. 2. Main dimensions of the lifting vessel

Main scale parameters	Parameter value (m)
Whole captain	238
Moulded beam	65
Moulded depth	21
Designed draft	12.5
Maximum draught for lifting operation	16.5

Table 3 provides the empty ship weight for the lifting vessel and centre of gravity position. The origin of the coordinate system applied here is at the intersection of the base plane, midship vertical plane, and stern bulkhead. In addition, each vessel design incorporates multiple lifting arms to enable diverse dual-vessel lifting schemes. A 5,000-ton stern-mounted offshore crane is included to independent heavy marine capabilities and to support dual-vessel operations. The weight of the offshore crane is calculated as part of the weight of the empty vessel, while the weight of the lifting system is calculated together with the weight of the block as the load weight.

Tab. 3. Empty ship weight for the lifting vessel and centre of gravity position

Object	Mass (ton)	Area coordinates (m)		
		X	Y	Z
Empty ship	57300	123.77	3.25	22.20

The typical topside module information is selected as the target analysis block. Information on a typical topside module is given in Table 4. The environmental conditions are selected based on a previous sea state information survey and window period analysis in the Beihai area. Environmental information is shown in Table 5.

Tab. 4. Typical topside module data

Name	Weight	Centre of gravity	Air gap	Lifting point spacing	Lifting arm overhang (m)	Overall dimensions
	(ton)	(m)	(m)	(m)		l×w×h (m)
Typical blocks	30,000	18.3	28.0	45.0	8.0	110.0×36.0×40

Tab. 5. Environmental information

Environmental condition	Numerical value	Remark
Wind velocity (m/s)	10	NPD wind spectrum
Flow velocity (m/s)	1	Contour of constant flow
Wave (m)	1–2.5	JONSWAP wave spectrum
Maximum inclination angle of lifting arm (deg)	1	—

By substituting the above parameters into Eq. (17), the moment of inertia of the free surface can be calculated as 1,123,776 ton·m. The stability analysis model is established as shown in Fig. 14, and the wind profile is established to determine the wind surface area as shown in Fig. 15.

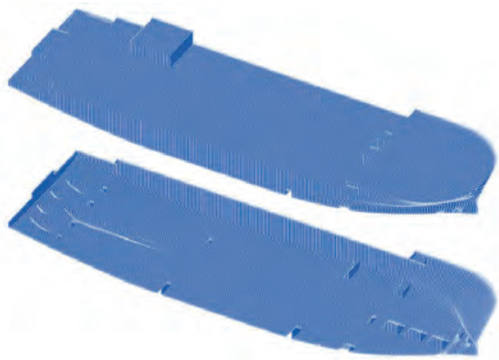

Fig. 14. Model of the lifting ship

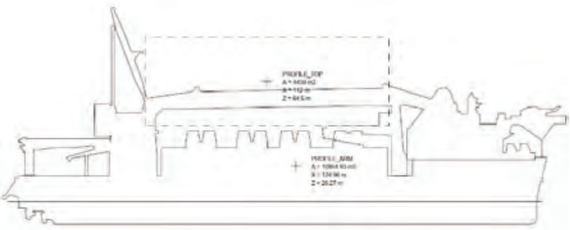

profile for lifting operation

T (m)	A (m2)	Z (m)	T (m)	A (m2)	Z (m)	T (m)	A (m2)	Z (m)
11.0	12746.4	38.0	13.2	12225.6	38.2	15.4	11699.0	38.4
11.2	12699.6	38.0	13.4	12177.7	38.2	15.6	11651.2	38.5
11.4	12652.7	38.0	13.6	12129.7	38.2	15.8	11603.4	38.5
11.6	12605.6	38.0	13.8	12081.8	38.2	16.0	11555.7	38.5
11.8	12558.5	38.0	14.0	12033.9	38.3	16.2	11508.0	38.5
12.0	12511.3	38.1	14.2	11986.0	38.3	16.4	11460.3	38.6
12.2	12464.1	38.1	14.4	11938.1	38.3	16.6	11412.6	38.6
12.4	12416.8	38.1	14.6	11890.2	38.3	16.8	11365.0	38.6
12.6	12369.3	38.1	14.8	11842.4	38.4	17.0	11317.3	38.6
12.8	12321.6	38.1	15.0	11794.6	38.4			
13.0	12273.6	38.2	15.2	11746.8	38.4			

Fig. 15. Wind profile under the lifting conditions

STABILITY ANALYSIS OF THE MULTI-BODY COLLABORATIVE OPERATION SYSTEM

Intact and loss-of-hook stability for multi-body collaborative operation system are analysed. We refer to the International Ship Integrity Stability Rules 2008 (hereinafter referred to as the 2008 IS CODE), and specifically the standard requirements for 'Lifting Operations under Environmental and Operational Constraints' and 'Sudden Loss of Hook Load'.

(1) The specific requirements for the integrity and stability of lifting operations are as follows, and are illustrated in Fig. 16:

(i) The freeboard deck cannot be submerged.

(ii) $A_{RL} \geq 1.4A_{HL}$

(iii) The minimum area under the curve of the restoring force arm from the equilibrium angle φ_1 to φ_2 the water inlet angle φ_f or 20° is at least equal to 0.03*mrad*.

Here, A_{RL} is the area under the curve of the restoring force arm from the equilibrium angle φ_1 to φ_2; A_{HL} is the area under wind tilt arm curve from the equilibrium angle φ_1 to φ_2.φ_2 is the minimum value of the second intersection of the water inlet angle, the stability disappearance angle, and two curves.

(2) The specific requirements for sudden loss of stability of the hook load are as follows:

Ships engaged in lifting operations and with reverse ballast should be able to withstand the sudden loss of hook load. Since the hook load may be applied to the most unfavourable point of the ship (i.e. with the maximum overturning moment), the area under the restoring arm curve on the opposite side of the crane is larger than the area on the side of the crane. For non-shielded waters, the following conditions need to be met, as shown in Fig. 17: $Area_2 > 1.4Area_1$.

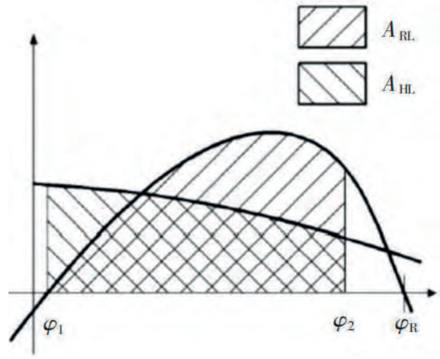

Fig. 16. Intact stability criteria under environmental and operational constraints

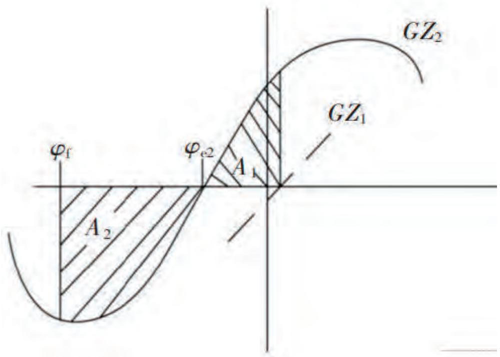

Fig. 17. Stability criterion in the case of heavy object loss

GZ_1 is the resilience arm curve considering the influence of heavy moudle and ballast water before the loss of hook ; GZ_2 is the resilience arm curve considering the influence of ballast water after the loss of hook ; φ_{e2} is the static balance angle after loss of hook, the water inlet angle φ_f is the small value of the second intersection point of the restoring force arm curve and the heeling force arm curve.

Fig. 18 shows the loading conditions for the two-ship lifting operation, and the results of an intact stability analysis under these conditions are shown in Fig. 19. It can be seen from Fig. 19(a) that the statistical angle is 0.1° and the dynamic angle is 28.5°. MOM denotes the heeling moment. Because the environmental is mild, so the overturning moment is small. Tables 6 and 7 present the results of an intact stability analysis and uncoupling stability analysis, respectively.

The deck immersion angle is found to be 7.619° and the static angle is 0.1°, meaning that the deck will not be submerged. As shown in Fig 19, we have Arl/Ahl = a/b = 0.3305/0.0063 = 52.46l >= 1.4, and A = 0.2637 ≈ 0.264 >= 0.03. Fig. 19 and Table 7 also give a value of $A1/A2$ = a/b = 1.585 > 1.4. The angle of static equilibrium after loss of the crane load is zero and the position of opening immersion is 0.425°, so the openings will not be immersed when the ship is in the equilibrium position after losing the hook.

Tab. 6. Results of an intact stability analysis

Loading condition	Deck not submerged		Area ratio ***Arl/Ahl*>=1.4**		Area not less than 0.03		Result
	Required (deg)	Actual (deg)	Required	Actual	Required (mrad)	Actual (mrad)	
Dual-vessel lifting	7.619	0.110	1.4	52.46	0.03	0.264	Pass

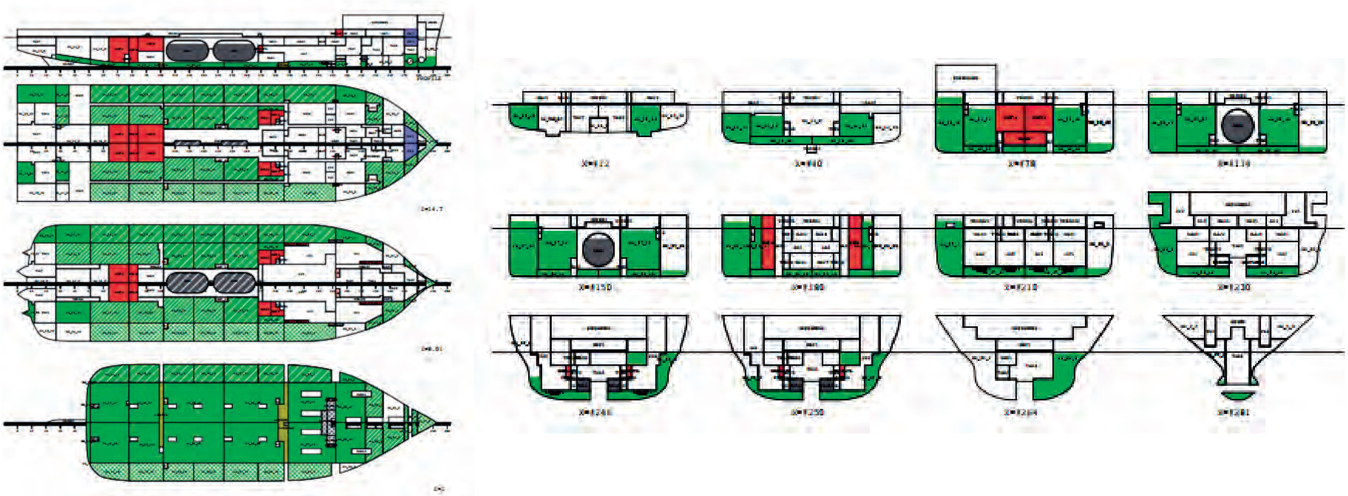

Fig. 18. Dual-vessel lifting and loading conditions

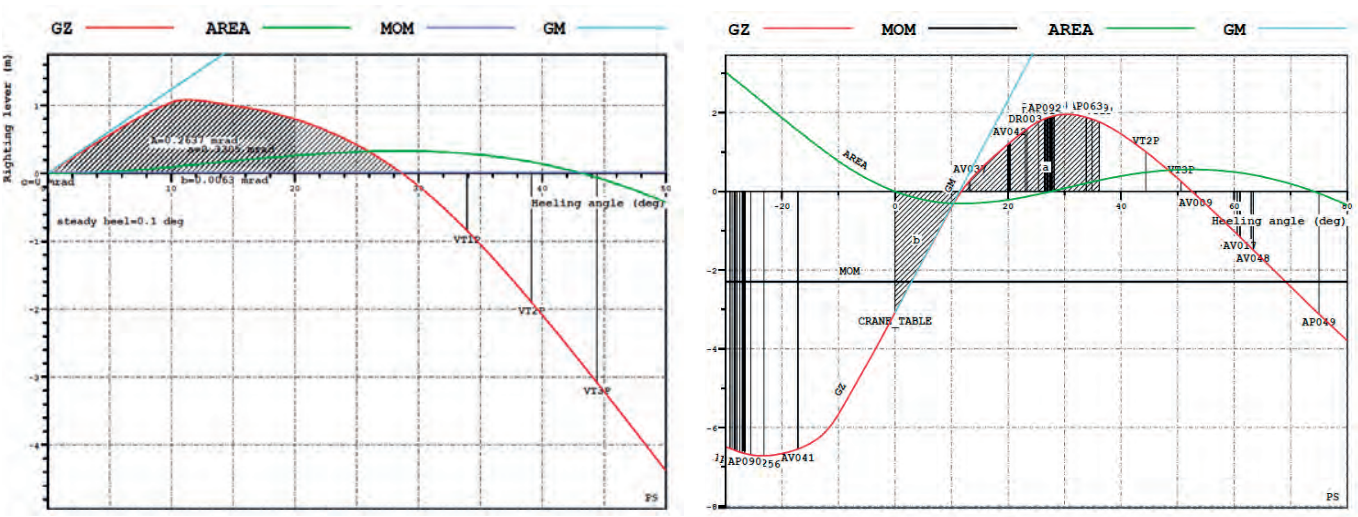

(a) (b)

Fig. 19. Results of a dual-vessel lifting stability analysis:
(a) intact stability analysis results; (b) decoupling stability analysis results

Tab. 7. Results of a loss of hook stability analysis

Loading condition	Area ratio after loss of hook ***A1/A2***>1.4		Equilibrium position without immersion of openings		Result
	Required	Actual	Required	Actual	
Loss of hook	1.4	1.585	0	0.425	Pass

The verification results demonstrate that the proposed dual-vessel cooperative approach to assembly and disassembly operations, in which we use multi-arm connections with motion compensation, meets the stability performance requirements for lifting a 30,000 ton topside module. The stability analysis method presented in this paper enables a stability evaluation of the multi-body cooperative operation system. Comprehensive stability checks were conducted on the vessels, lifting system, and topside module.

CONCLUSION

The aim of this paper was to address the limitations associated with current offshore assembly and disassembly equipment by proposing a new approach based on multi-arm lifting connections with integrated motion compensation capabilities. From hydrostatic considerations, we develop an equivalent simplified overall stability analysis method for a multi-body system, which enables checks of the intact and loss-of-load stability of the dual-vessel collaborative operation system. In this system, multiple lifting arms connect the lifting vessels to the topside module, and integrated motion compensation is applied between components. The main conclusions of the study are as follows:

(1) Although rigid connections can offer excellent stability and safety, realising these in practical offshore engineering scenarios poses considerable challenges, especially when decommissioning aged platforms, due to issues with stiffness and resistance. This paper has put forth a lifting arm motion compensation system to help resolve such difficulties. The proposed mechanism aims to relieve the bending moments at the connection point between the lifting apparatus and topside module, and to prevent the transfer of wave loads impacting the lifting vessel, particularly via torque stresses on the lifting arms and topside assembly. By offsetting the relative motion, this approach endeavours to guarantee the structural soundness of the topside module. Our solution seeks to overcome the technical barriers hampering renewal and disassembly operations involving outdated fixed offshore structures.

(2) A formula is derived to allow us to calculate the transverse ballast water allocation required to balance the torque generated by the increase in the lifting load. The variation in the ballast water needed to cope with the tidal changes in the working sea area is also calculated. Through an analysis of the tilting moments imparted on the lifting arms and the lifting loads exerted on the vessel, and considering the effects of the tide on the disassembly operation, the design of the cabin layout and ballast water system was optimised. The results showed that equipping the single vessel with seven groups of anti-heeling tanks and 14 anti-heeling pumps was an effective approach. The maximum volume of ballast water transfer was determined to be approximately 10,900 m^3, where each pump had a flow rate of 1,500 m^3/h. This optimised ballast water system design will help ensure safe and stable heavy lifting operations in variable tidal environments.

(3) Intact and loss-of-hook stability analyses were conducted for a dual-vessel heavy lifting configuration, where the overturning moment imparted by inclination of the module was incorporated into the loading calculations as an inertial moment from free surface effects. The results demonstrated that lifting a 30,000-ton topside module using this approach would satisfy all stability criteria under both intact and loss of hook stability conditions. The results for the intact stability exceeded the calibration thresholds by a wide margin, and the loss of hook stability was also above the required levels. This confirms that the proposed lifting configuration and methodology can safely perform heavy lifting operations for very large modules, while effectively achieving both intact and loss-of-hook stability throughout the operation. Our approach was therefore validated in this analysis, and provides an efficient solution for offshore disassembly of mega-scale oil and gas infrastructure modules.

In summary, this paper has presented a dual-vessel lifting approach with motion compensation, which was validated using stability analysis. Our scheme addresses the shortcomings of current systems and enables the optimisation of collaborative offshore module disassembly operations.

Author contributions: Conceptualization, Dejiang Li,Shumin Li and Qiuotng Tan; Data curation, Qiang Fu and Chao Hu; Formal analysis, Jiwei Liu and Yuhai Sun; Investigation, ShuMin Li; Methodology, Dejiang Li,Shumin Li and Qiuotng Tan; Project administration, Chao Hu; Resources, ShuMin Li; Software, Qiuotng Tan; Validation, Jiwei Liu;Writing – original draft, Dejiang Li; Writing – review &editing, Qiuotng Tan.

Funding: This research was funded by the Shandong Province Major Project (No. 2021CXGCO10701), Research on key technology and equipment of double-ship lifting for super-large offshore structures (2021CXGC010701),General Project of Guangdong Province Department of Natural Resources to Promote High-quality Economic Development (No. GDOE[2020]026, No. GDOE 2022]30).

Institutional Review Board Statement: Not applicable.
Informed Consent Statement: Not applicable.
Data Availability Statement: Not applicable.
Conflicts of Interest: The authors declare no conflict of interest.

REFERENCES

1. Pang R D, Li Y D, Ding B, Sun T, Li Y F, Liu P. Analysis of the adaptability of offshore platform structure type and floating lifting method. Ocean Engineering Equipment and Technology 2020.

2. Hu Z G. Analysis of offshore platform demolition operation risk and prevention. Chemical Equipment Technology 2019, doi: 10.16759/j.cnki.issn.1007-7251.2019.10.014.

3. Vidal P D C J et al. Decommissioning of offshore oil and gas platforms: A systematic literature review of factors involved in the process. Ocean Engineering 2022, doi: 10.1016/j.oceaneng.2022.111428.

4. Jin X J, Research and practice of large offshore platform floatover technology. Science Press; 2017.

5. Sun L M. The development of China's offshore lifting and salvage operation and its basic equipment large crane ship. Marine Engineering 2013, doi: 10.13788/j.cnki.cbgc.2013.01.023.

6. Yang Y. A brief analysis of the history of China's offshore oil exploration and development. China University of Geosciences (Beijing); 2017.

7. Li C Y, Yao H, Yu B L. Heavy-duty full-revolving crane ship: A sharp weapon for marine resource development. Shanghai Informatization 2017.

8. Liu Z Q. The world's largest semi-submersible crane ship docked at the port of Rotterdam. Navigation 2020.

9. J. Du Bois. Improved mode of constructing, setting, and removing bridge. U.S. Patent 36,606, October 1862.

10. Wang L X. The application of VERSATRUSS lifting system in ocean engineering. Petroleum Engineering Construction 2007.

11. Bjørheim P S. A feasibility study of the Versatruss system. Master's thesis, University of Stavanger, 2015.

12. Rassenfoss S. Aging offshore fields demand new thinking. Journal of Petroleum Technology 2014, doi: 10.2118/1114-0050-JPT.

13. Xu X, Yang J M, Li X. The development of floatover installation and its key technology. China Offshore Platform 2012.

14. Phillip A A, Larry E F, Graham J B, and Osborne M D. A new integrated deck concept. OTC Offshore Technology Conference (OnePetro) 1980, doi: https://doi.org/10.4043/3879-MS.

15. Blight G J, Rohde H K, Abbott P A. Method and apparatus for installing integrated deck structure and rapidly separating same from supporting barge means.Fremgangsmaate for tilveiebringelse av en offshore-konstruksjon. Norway: N. p., 1984.

16. Karsan D I, Blight G J, Farmer L E. Method and apparatus for forming integrated deck sub-structure assembly including arch-vessel passage means. U.S. Patent No. 4,242,011. 30 Dec. 1980.

17. Blight G J. Method and apparatus for installing deck structures entailing composite shock absorbing and alignment aspects. U.S. Patent No. 4,252,468. 24 Feb. 1981.

18. Mcculley Russell. Technology and economics align to boost FLNG. Offshore 2013.

19. Ji C, Halkyard J. Spar deck float-over feasibility study for West Africa environment condition. In 25th International Conference on Offshore Mechanics and Arctic Engineering 2008, doi: 10.1115/OMAE2006-92157.

20. Xu X. Study on coupling dynamic response of float-over installation system. Shanghai Jiao Tong University, 2016.

21. Liu G, Li H. Offshore platform integration and floatover technology. Springer Tracts in Civil Engineering; 2017, doi: 10.1007/978-981-10-3617-0.

22. Batista M D E, Vellasco P, Lima D O R L, Tubular structures XV. In Proceedings of the 15th International Symposium on Tubular Structures, Rio de Janeiro, Brazil, 27-29 May 2015.

23. Van Vuuren F. Vessel motion prediction for *Pioneering Spirit* in shallow water. Delft University of Technology; 2018.

24. Wilson F, Munro-Kidd A. Caspian challenge for marine installation. In Offshore Technology Conference 2008, doi: https://doi.org/10.4043/19237-MS.

25. Iain. SeaMetric International. Energy, Oil & Gas magazine. 2008. Retrieved from https://energy-oil-gas.com/news/seametric-international/.